

CREEP BEHAVIOR OF 1Cr0.5Mo STEEL . PART 1 – CHARACTERIZATION AND DATA PARAMETERIZATION IN THE VIRGIN CONDITION*

Levi de Oliveira Bueno¹

Abstract

Constant stress testing was used for characterization of creep behavior of a 1Cr0.5Mo steel plate in the virgin condition. The tests were performed on creep machines equipped with Andrade-Chalmers type profiles, high sensitivity SLVC transducer extensometry, high stability temperature controllers, and facilities for monitoring the creep curves with an automatic data logging system. Ten creep machines of this type were used in this research, in an experimental work that lasted for one year. Three temperature levels were selected: 538, 565 and 593°C, with stress in the range from 69 to 258 MPa producing rupture times varying from 8 to about 4908 h. The creep curves were all followed with great scrutiny using data logger scanning rates which enabled storing thousands of readings in each case. The experimental analysis involved measurements of minimum creep rate, rupture time and final elongation at rupture. The data were analyzed according to the classical phenomenological / physical relations (Norton, Arrhenius, Zenner-Hollomon, Monkman-Grant) and also considering five traditional parameterization methodologies (Larson-Miller, Orr-Sherby-Dorn, Goldhoff-Sherby, Manson- Haferd and Manson-Succop). Comparisons are presented among the possibilities of data extrapolation from five different methodologies. Comparison is also made with creep results mentioned in literature for the same material in the virgin condition.

Keywords: 1Cr0.5Mo steel - virgin condition; constant stress creep; creep relations; data parameterization.

¹ *PhD/Materials Engineering, Associate Professor / Retired from Materials.Engineering Dept. / UFSCar, São Carlos-SP. Now at STM-Systems for Testing of Materials Ltda., São Carlos-SP, Brazil.*

1 INTRODUCTION

1Cr0.5Mo steel is largely used in the manufacture of high temperature components, especially boilers, waterwall tubes, drums, headers, superheater/reheater tubes, steam pipes, etc, as well as for pressure vessels and catalytic reactors. Temperature operation of 1Cr0.5Mo steels in such systems is situated usually in the range from 550 to 605°C. Monitoring the state of damage caused by creep in these components is of paramount importance.

During a scheduled shutdown, for maintenance, a section of a heavy wall plate was extracted from a FCC (Fluid Catalytic Cracking) Reactor of a petrochemical plant for inspection. The plate was manufactured with 1Cr0.5Mo steel and operated for about 17 years (~150.000 h) at a nominal temperature of 565°C and one of the main concerns was the determination of its creep properties within a work program for its residual life assessment.

A similar plate of the same material, in the virgin condition, was also considered for a comparative study. The characterization of the creep behavior of the virgin and ex-service materials was performed using constant stress creep machines having high sensitivity instrumentation in a British creep laboratory.

Due to the large amount of data generated in this project, in the present work (Part 1) only the results on the virgin material will be presented. In another article [1] of this conference (Part 2) the results on the ex-service material are also described and compared with results on the virgin material. The main objective in these two articles is the determination of parameters related to creep behavior and procedures of data extrapolation in the two versions of the material.

Another important objective of the work was the analysis of all these data according to the Theta-Projection methodology proposed by Evans and Wilshire [2,3,4]. However, due to the large amount of information on this subject, the results of that work will be presented in a future publication.

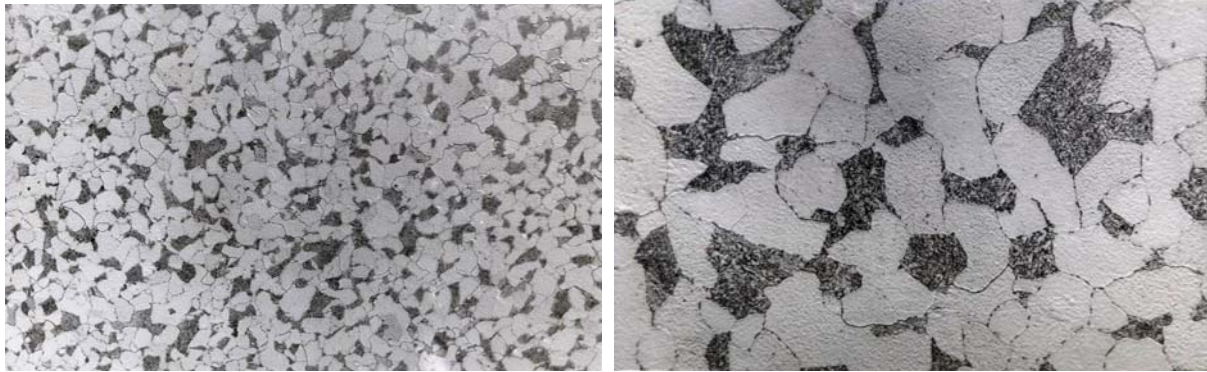
2 MATERIALS AND METHODS

The material used in this research is a typical 1Cr0.5Mo steel type A387 Grade 12CL2.

Figures 1a and 1b show the microstructure of the material in the virgin condition, consisting of a structure of grains of about 80% pro-eutectoid ferrite and 20% tempered bainite.

Creep specimens with cylindrical shape were obtained from the virgin sample, having shoulders with thread M12x1.75, gauge-length $L_0 = 25\text{mm}$ and diameter $D_0 = 6.25\text{mm}$. Creep tests were carried out in *constant stress* type Dennison machines having load-levers equipped with Andrade-Chalmers profiles (cams). The furnaces operated with micro-processed temperature controllers capable of maintaining the temperature within $\pm 1^\circ\text{C}$ during the tests. High temperature extensometers employing SLVC transducers were used to monitor the elongation of the specimens. The readings of elongation and time were collected by an ASL Data Logger system that could be programmed to make scanning in the whole group of creep machines at appropriate time intervals. Twenty three specimens of the ex-service material were tested using a set of 10 creep machines that operated during about 20820 h.

Three levels of temperature were selected for this research: 811K (538°C), 838K (565°C) and 866K (593°C).



a) [original magnification 100x]

b) [original magnification 400x]

Figure 1 – Optical micrographs of the material in the virgin condition.

The applied stresses varied in the range from: 69 to 258 MPa, producing rupture times lasting from about 8 to 4908 h.

The creep curves were all followed with great scrutiny using data logger scanning rates which enabled storing thousands of readings in each case. This was necessary for the analysis of the data according to the Theta-Projection methodology [2] which will be the subject of a future publication.

The analysis of the data relative to the present article (Part 1) involved determination of the variation of minimum creep rate, the rupture time, the final elongation of the specimens in terms of temperature and stress used in the tests.

3 RESULTS AND DISCUSSION

Figure 2a shows a plot of LOG(Stress) versus LOG(Rupture Time), i.e. the Loss of Creep Rupture Strength with Time exhibited by the material at the three temperature levels investigated.

Figure 2b shows the creep data plotted in the form of a Norton diagram, i.e. LOG(Stress) versus LOG(Rupture Time), used to verify the validity of the Norton relation: $\dot{\epsilon}_s = A'\sigma^n$ at a certain iso-temperature condition ($\dot{\epsilon}_s$ = Secondary or Minimum Creep Rate, σ = Applied Stress, with A' and n constants). Straight lines fitted to each set of iso-temperature data gives $n=6.0$ for 866K, $n=6.5$ for 838K and $n=6.9$ for 811K.

Figure 3a shows the creep data plotted in the form of an Arrhenius diagram, i.e. LN(Minimum Creep Rate) versus $1/T$, used to verify the validity of the relation: $\dot{\epsilon}_s = A'' \exp(-Q_c/RT)$ at a certain iso-stress condition ($\dot{\epsilon}_s$ = Secondary or Minimum Creep Rate, T = temperature, with A'' and Q_c (Apparent Creep Activation Energy) constants). Straight lines fitted to each iso-stress set of data produces an average value for the apparent creep activation energy of $Q_c = 389$ kJ/mol.

The data shown in Figure 2b in the form of a Norton diagram can be rationalized using the Zener-Hollomon parameter, defined as: $Z = \dot{\epsilon}_s \cdot \exp(-Q_c/RT)$, taking $Q_c = 389$ kJ/mol. As shown in Figure 3b, when LOG(Z) is plotted in terms of LOG(σ), the three iso-temperature sets of data of Figure 2b collapse in the form of a single reference curve, so that creep behavior is better expressed by: $Z = A''' \sigma^n$. It can be observed that this reference curve is not a straight line, i.e. the value of n is not constant, as the stress varies. In fact, in the lower range of stress the value of n is about $n \approx 5.5$ whilst in the higher range $n \approx 6.9$.

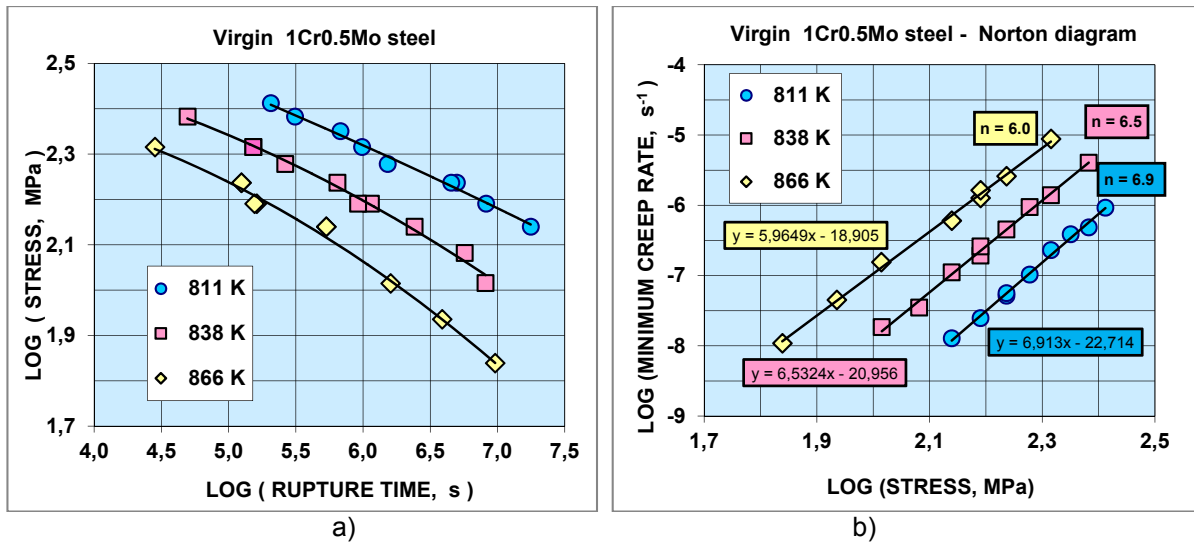


Figure 2 - a) Loss of Creep Rupture Strength with Time; b) Norton diagram.

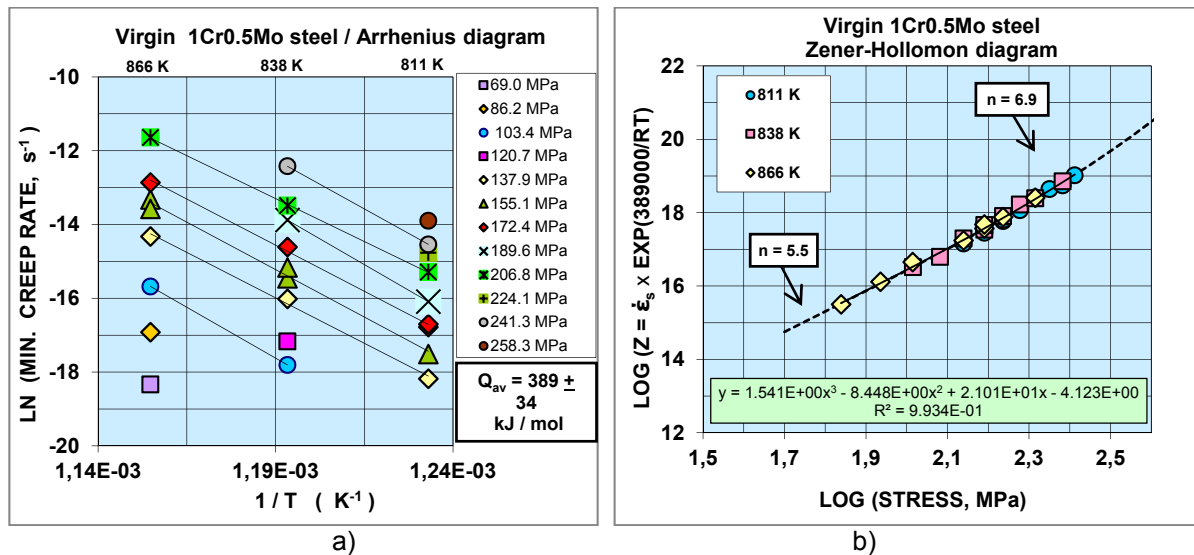


Figure 3 - a) Arrhenius diagram, b) analysis of the data using the Zener-Hollomon parameter.

A 3rd degree polynomial was well fitted to the data, although it not at all reliable to be used for extrapolation of the data much beyond the experimental data range.

Figure 4a shows the creep data plotted in the form of the Monkman-Grant diagram, so as to verify the validity of the Monkman-Grant relation: $\dot{\epsilon}_s \cdot t_r^m = K$ (t_r = rupture time, m and K constants). The present data produced the value of $m=1.0356$ and $K=0.346$. The Monkman-Grant plot represents a kind of natural parameterization of the data of $\text{LOG}(\dot{\epsilon}_s)$ in terms of $\text{LOG}(t_r)$. In this article we suggest the possibility of rationalization of the Monkman-Grant plot using the Zener-Hollomon parameter, instead of Minimum Creep Rate in the Y-axis, and the Temperature Compensated Rupture Time, instead of Rupture Time in the X-axis, i.e. $\Theta = t_r \cdot \exp(-Qc/RT)$. The new Monkman-Grant relation could be expressed now by:

$$Z \cdot \Theta^{m'} = K^* \quad \text{with } m' \text{ and } K^* \text{ constants} \quad (1)$$

Therefore Equation 1 considers parameterization of the data in the X and Y axis.

Figure 5a shows the creep data plotted in the space $\text{LOG}(t_r)$ versus $1/T$. This is the kind of graph that must be organized to inspect the possibility of parameterization according to the methods of Larson-Miller, Orr-Sherby-Dorn and Goldhoff-Sherby [5].

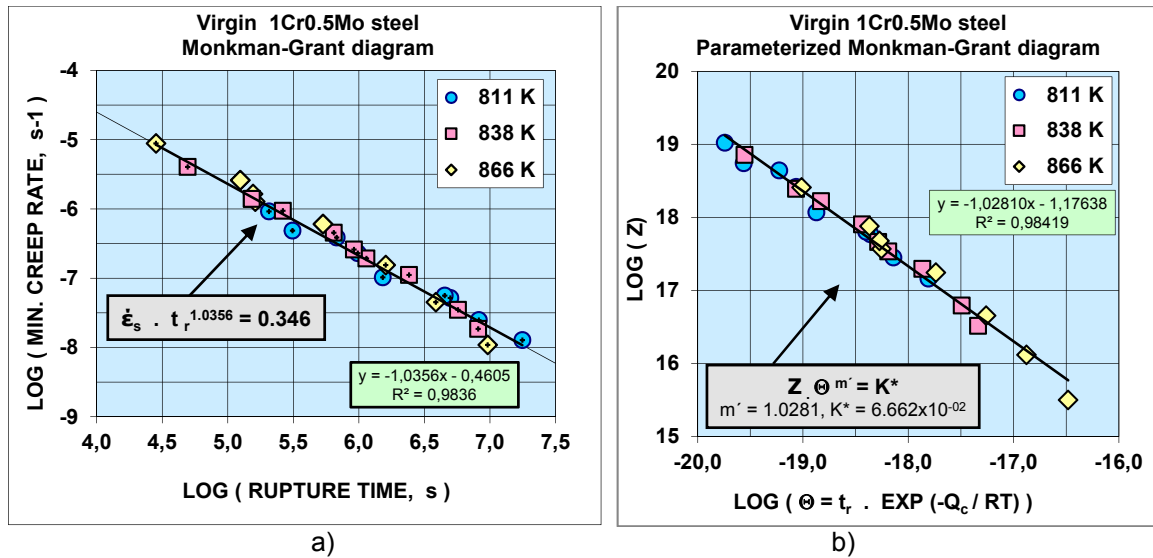


Figure 4 – a) Monkman-Grant diagram; b) rationalization of the Monkman-Grant diagram using the Z and Θ parameters.

Figure 5b shows the same data plotted in the space $\text{LOG}(t_r)$ versus T , which is used for exploring the possibility of parameterization by the methods of Manson-Haferd and Manson-Succop [5]. In both cases, the least-square procedure of Manson-Mendelsohn [6] was used to derive the values of the constants of each method. The parameters of these methods are defined by the following relations:

Larson-Miller Parameter: $\text{LMP} = T[C + \text{LOG}(t_r)]$ (2)

Orr-Sherby-Dorn Parameter: $\text{OSDP} = \text{LOG}(t_r) - A/T$ (3)

Goldhoff-Sherby Parameter: $\text{GSP} = - [\text{LOG}(t_r) - \text{LOG}(t_r)^*] / [1/T - (1/T)^*]$ (4)

Manson-Haferd Parameter: $\text{MHP} = - [(T - T^*) / (\text{LOG}t_r - \text{LOG}(t_r)^*)]$ (5)

Manson-Succop Parameter: $\text{MSP} = \text{LOG}(t_r) - BT$ (6)

where C, A, $\text{LOG}(t_r)^*$, $(1/T)^*$, T^* and B are characteristic constants of each method.

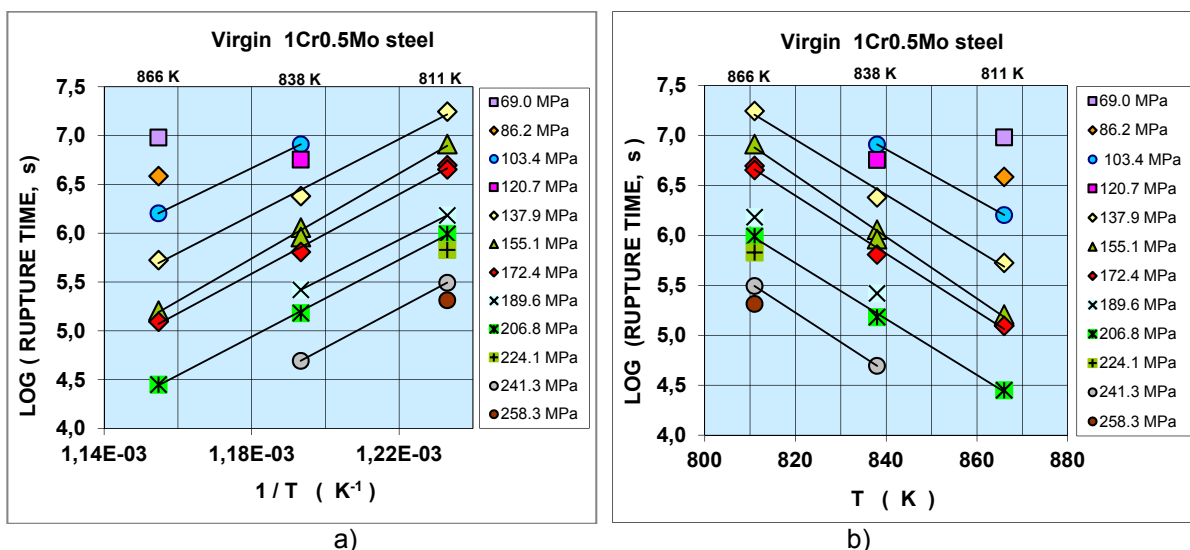


Figure 5 - Plot of $\text{LOG}(t_r)$ versus $1/T$ to verify possibility of parameterization by the methods of Larson-Miller, Orr-Sherby-Dorn and Goldhoff-Sherby; plot of $\text{LOG}(t_r)$ versus T to verify possibility of parameterization by the methods of Manson-Haferd and Manson-Succop.

The definition of the Manson-Haferd parameter given here is somewhat different from the original formulation: $MHP = (\text{LOG}t_r - \text{LOG}(t_r^*)) / (T - T^*)$ which produces negative numbers. Calculation according to Equation 4 gives always positive numbers which are more convenient. This is the formulation adopted by some authors, as G.E.Dieter, for instance [7].

Figure 6 presents the 5 parameterization curves obtained with this analysis. The constants involved in each method are specified in each figure. In each case, low degree polynomials (2nd degree) were fitted to the data. The quality of fit of each methodology can be judged from the values of the corresponding correlation coefficients R^2 . The best fit was achieved with the Orr-Sherby-Dorn and Larson-Miller analysis (both with $R^2 = 0.99219$). In the sequence comes the analysis with: Manson-Succop ($R^2 = 0.99135$), Manson-Haferd ($R^2 = 0.98790$) and Goldhoff-Sherby ($R^2 = 0.97507$) methodologies.

The parameterization curve of the Orr-Sherby-Dorn methodology was selected for extrapolation of the data of the ex-service material. The constant A determined by the Manson-Mendelsohn analysis [6] in this methodology was $A = 20271$.

The predictive quality of the Zener-Hollomon analysis in predicting the minimum creep rate data is shown in Figure 7a. In the same way, the predictive quality of the Orr-Sherby-Dorn analysis in predicting the rupture time data is shown in Figure 7b. It can be noticed that in both cases the agreement of the iso-temperature lines at 811K, 838K and 866K with the corresponding experimental points is excellent. The better performance of the Orr-Sherby-Dorn analysis in the present results also agrees with the parameterization of the Monkman-Grant data (Figure 4a) in terms of Z as function of the Temperature Compensated Rupture Time:

$$\Theta = t_r \cdot \exp(-Q_c/RT) \quad (7)$$

as proposed in this article. The Θ parameter is closely related to the OSDP, since:

$$\text{LOG}(\Theta) = \text{LOG}(t_r) - \text{LOG}(e) \cdot (Q_c/RT)$$

and therefore:

$$\text{LOG}(\Theta) = \text{OSDP} \quad 7a$$

and

$$A = Q_c \cdot \text{LOG}(e)/R \quad 7b$$

Since $A=20271$ for the ex-service material $\rightarrow Q_c = 388$ kJ/mol, a value that is close to $Q_c=389$ kJ/mol determined from the Arrhenius diagram in Figure 3a.

It is important to emphasize that the use of the extrapolation curve in Figure 6b is reliable only for predictions up to about 50,000 h, i.e. considering the maximum of one LOG cycle beyond the experimental range attained in this work. The extrapolation can also be made more reliable if instead of a 2nd degree polynomial a more appropriate function is used to fit the data in Figure 6b, such as the Spera function, for instance [8].

Figure 8a shows the variation of the initial strain upon loading of the specimens with stress and temperature, as detected by the creep extensometers. There is a considerable degree of scatter in such kind of data and the interrupted line represents an average trend through all the points. This curve reflects the variation of the elastic modulus with temperature, although for the higher stress levels in each temperature there is the possibility of occurrence of plastic strain in addition to the elastic strain.

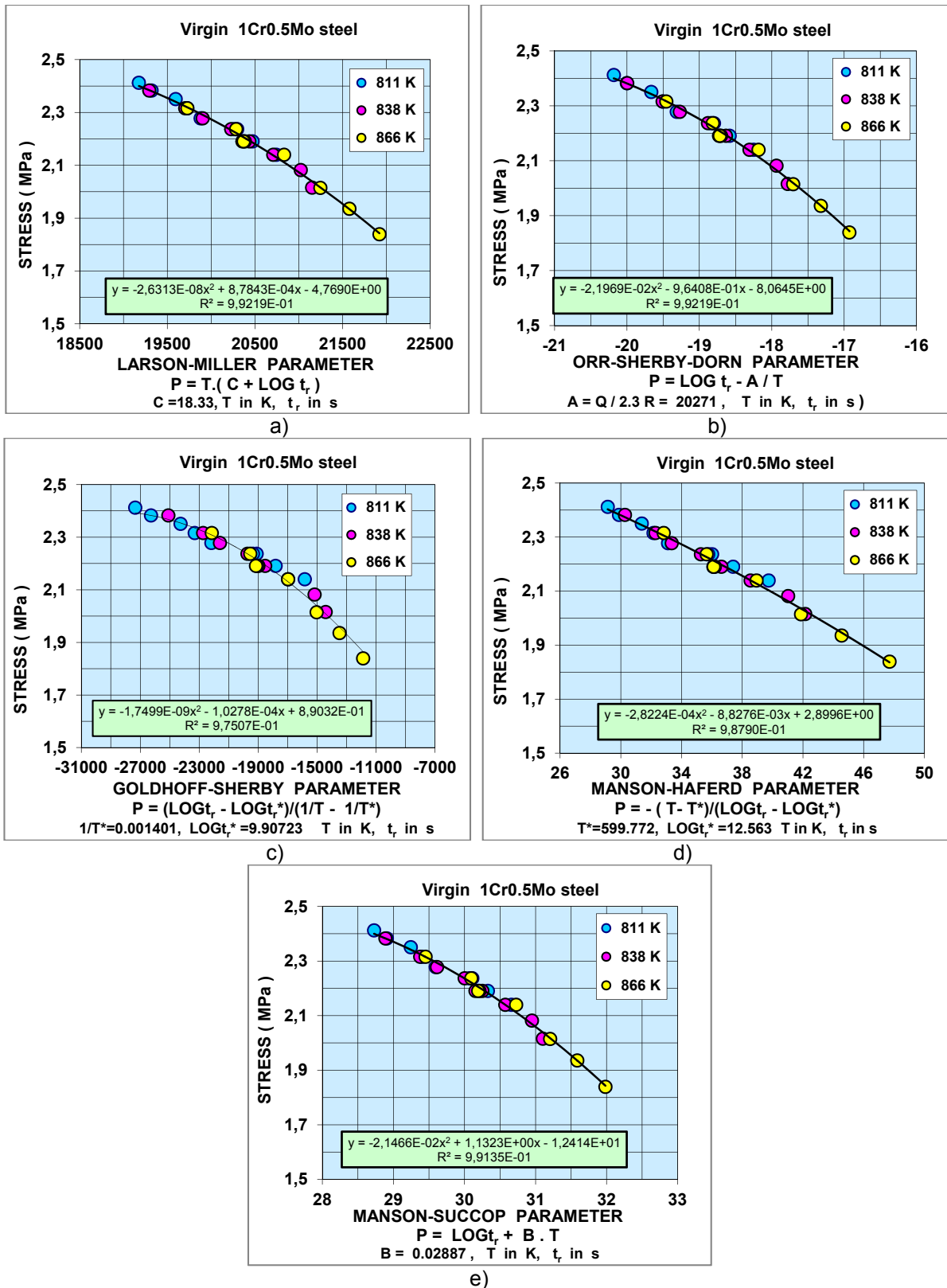


Figure 6 - Parameterization by the methods of: a) Larson-Miller; b) Orr-Sherby-Dorn; c) Goldhoff-Sherby; d) Manson-Haferd; e) Manson-Succop.

Figure 8b depicts the variation in creep ductility (represented by the final percentage elongation detected by the extensometers, i.e. the last point in each creep curve) with stress and temperature. The creep ductility of the virgin material varies in a range from about 20% to 45%, also with a considerable degree of scatter.

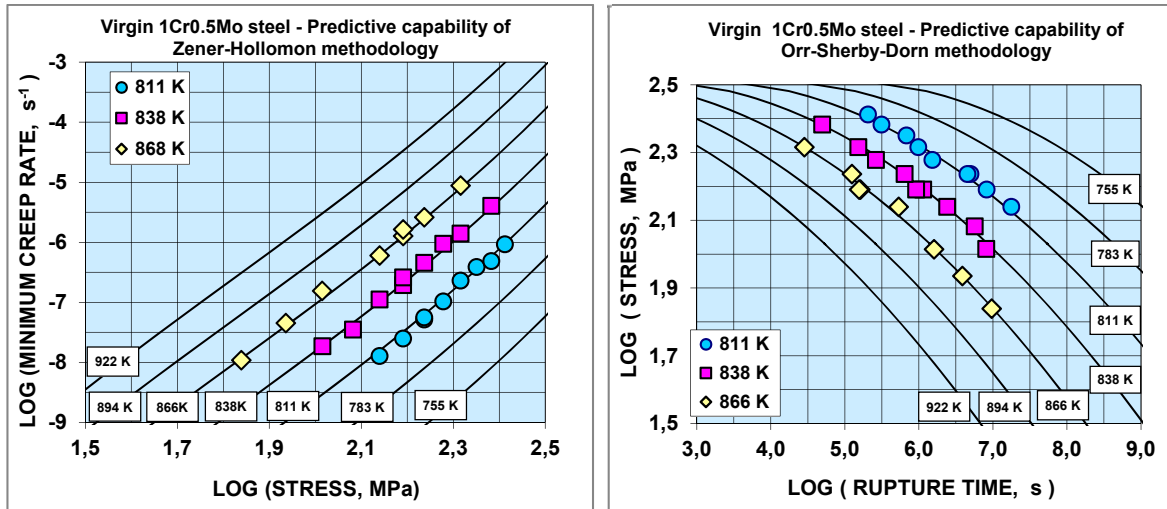


Figure 7 – Predictive Capability of the: a) Zener-Hollomon parameterization in the Norton diagram; b) Orr-Sherby-Dorn parameterization in the Loss of Strength with Rupture Time diagram.

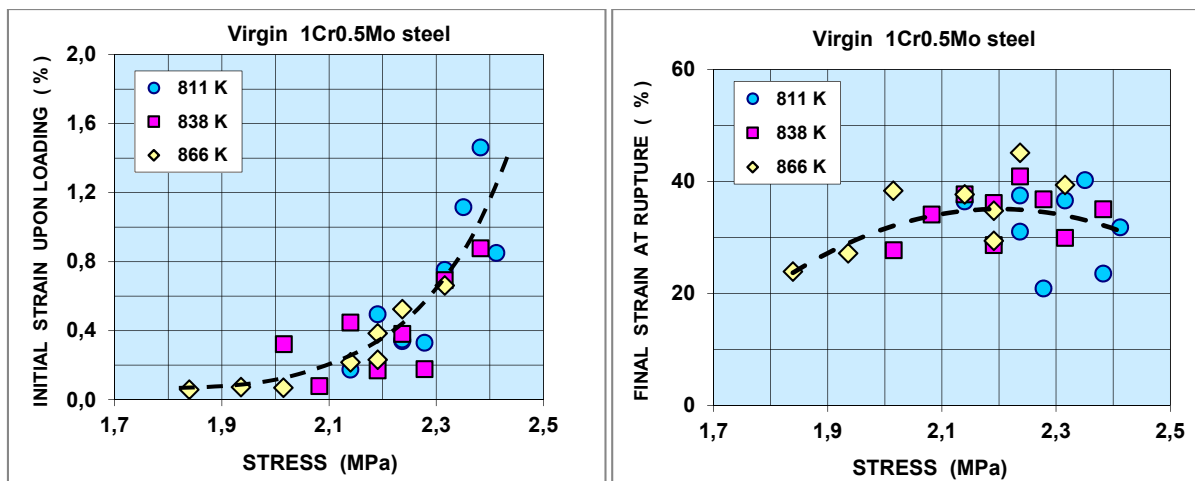


Figure 8 – a) Variation of the initial strain upon loading with stress and temperature; b) Variation of creep ductility with stress and temperature, for virgin 1Cr0.5Mo steel.

The average line through the points (interrupted line in Figure 8b) increases monotonically from 20% up to a maximum of about 35% at 140 MPa and decreasing to about 30% at 250 MPa.

Figure 9a presents results from NIMS-National Institute for Materials Science, Japan, for 1Cr0.5Mo steel [9], relative to the Loss of Strength with Rupture Time in four temperature levels: 500°C, 550°C, 600°C and 650°C, involving creep tests lasting up to about 30 years. Figure 9b shows the same results analyzed according to the Manson-Haferd method, with MHP defined according to its original formulation. The focal point of NIMS data has coordinates $T^*=510K$ and $t_r^*=1.22 \times 10^{13} \times 3600 = 4.392 \times 10^{16}s$ whilst in the present work it was found $T^* \approx 600K$ and $t_r^* = 3.656 \times 10^{12}s$. The great difference between the t_r^* values might be due the much larger values of rupture times attained in NIMS work. Figures 9a and 9b were adapted from Figures 1 and 4 mentioned by Wilshire and Sharning [10] who reanalyzed NIMS data for rationalizing creep extrapolation procedures.

Figure 10 presents a comparison between results of this work and NIMS Data for 1Cr0.5Mo steel, using in both cases the same Manson-Haferd constants for T^* and t_r^* . The NIMS curve was constructed from Figure 9b using the average points of the

data in each stress level. It is interesting that even with the NIMS Manson-Haferd constants the results of the present work also show good parameterization. At the higher stress levels (above 130MPa approximately), NIMS material exhibits a considerable higher creep strength than the material of the present research. However, there is a trend of coincidence with the NIMS data at the lower stress levels. As pointed out by Wilshire and Scharring [10], in the NIMS data analysis, Norton exponents decreases from $n=14$ to $n=3$ and activation energy decreases from $Q_c=490\text{kJ/mol}$ to $Q_c=280\text{kJ/mol}$. The material in the present work showed lower values for n and Q_c in creep tests with lower durations. NIMS data refers to 1Cr0.5Mo in the form of tubes for boilers and heat exchangers whereas the present version of the steel is a plate, as described in session 2. Figure 10a presents a comparison between the curves of Loss of Strength versus Rupture Time for NIMS and the present data at the various temperatures investigated in each work.

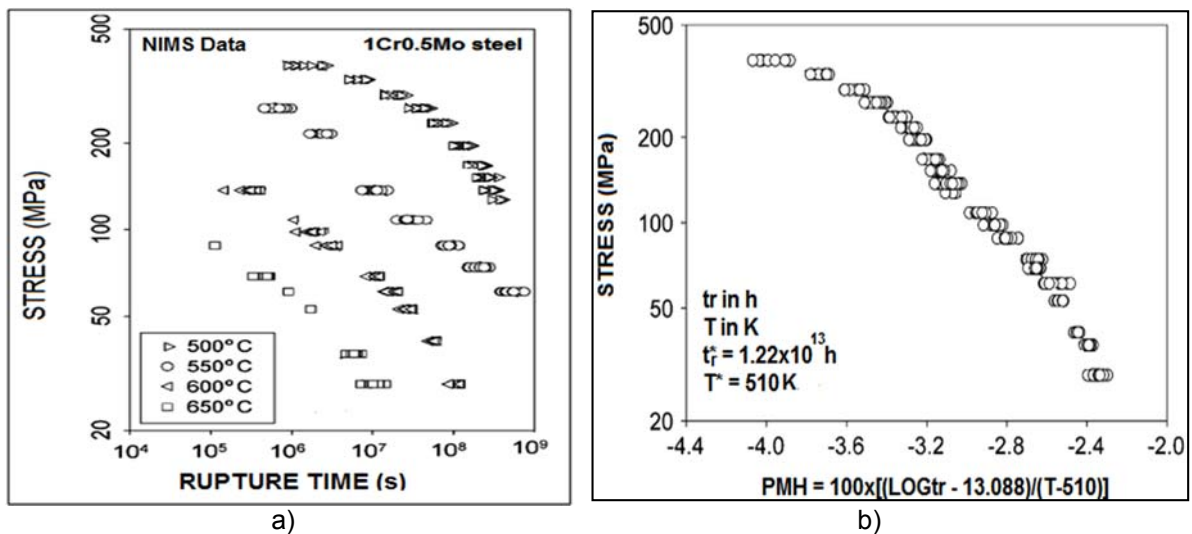


Figure 9 - NIMS Data for 1Cr0.5Mo steel: a) Loss of Strength with Rupture Time; b) Manson-Haferd parameterization. Obsv: Figures a) and b) adapted from Figures 1 and 4, respectively, in Ref. 9.

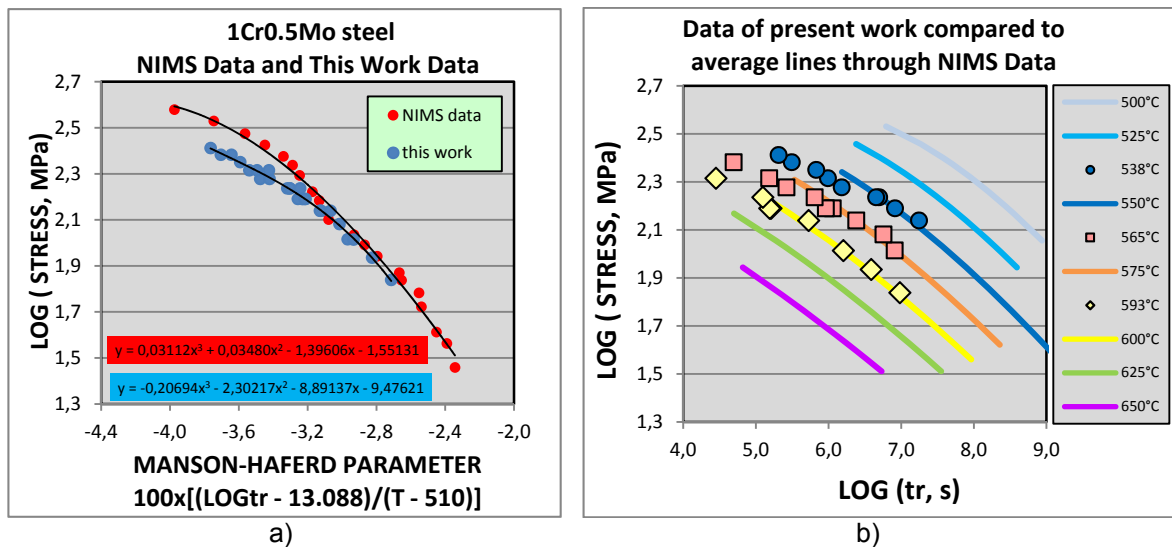


Figure 10 - Comparison of results of this work with NIMS Data for 1Cr0.5Mo steel: a) NIMS Data and This Work Data under Manson-Haferd parameterization; b) Loss of Strength with Rupture Time for NIMS Data and This Work Data.

4 CONCLUSION

The characterization of creep behavior of 1Cr0.5Mo steel in the form of plate type A387 Grade 12 CL2 produced the following results, for constant stress tests in the range from 69 to 258 MPa, at three temperature levels (811, 838 and 866K):

- a) Norton diagram produced the following n values for the material: $n = 6.0$, 6.5 and 6.0 for $T = 866\text{K}$, 838K and 811K , respectively.
- b) Arrhenius diagram indicated an average Apparent Creep Activation Energy $Q_c = 389 \pm 34$ kJ/mol for the material.
- c) Zener-Hollomon parameterization, with $Q_c = 389$ kJ/mol, was effective in transform Norton diagram in a single reference curve, with the stress exponent varying from $n = 5.5$ to $n = 6.9$ at the lower and higher stress levels, respectively.
- d) Monkman-Grant diagram produced values of $m = 1.0356$ and $K = 0.346$ in the relation: $\dot{\epsilon}_s \cdot t_r^m = K$, with $\dot{\epsilon}_s$ in s^{-1} and t_r in s.
- e) Monkman-Grant diagram can be parameterized using the Zener-Hollomon parameter and the temperature compensated rupture time: $\Theta = t_r \cdot \exp(-Q_c/RT)$, so that the relation: $Z \cdot \Theta^{m'} = K^*$ is valid with $m' = 1.2081$ and $K^* = 6.662 \times 10^{-02}$.
- f) Five methods from the traditional parameterization literature were tested with the present data and the best results were obtained with the Orr-Sherby-Dorn analysis, with a constant $A = 20271$ and Larson-Miller analysis with $C = 18.33$.
- g) Comparison of the results of this work with NIMS data on tubes for boilers and heat exchangers indicates that the 1Cr0.5Mo steel in plate form used in this research shows lower creep rupture strength for stresses higher than about 130 MPa, with a trend of coincidence with the NIMS data for stresses lower than 130 MPa.

Acknowledgments

The author acknowledges The Federal University of São Carlos and the Department of Materials Engineering for conceding a license of study in the UK and the provision of a grant by FAPESP-Fundação de Amparo à Pesquisa do Estado de São Paulo to support his stage at the Engineering Materials Department / Swansea University in Wales during two years. Acknowledgements are also due to Prof. Brian Wilshire for his permission to use 10 constant stress creep machines in this project at IRC-Interdisciplinary Research Center/USW and also to Dr. Miles Davis for his technical assistance during the experimental work in the Creep Laboratory. Special thanks are also due to José Cláudio Guimarães Teixeira from CENPES-Petrobrás, Rio de Janeiro (RJ), for supplying the samples of the material used in this research.

REFERENCES

- 1 Bueno LO. Creep Behavior of Service Exposed 1Cr0.5Mo Steel. Part 2 – Analysis based on the Theta Methodology approach. Proc. ABM Week 2015 – 70th ABM Annual Congress, 17–20 August, Rio de Janeiro (RJ), Brazil.
- 2 Evans RW, Wilshire B. Creep of Metals and Alloys. The Institute of Metals. London, UK, 1985.
- 3 Wilshire B, Scharning PJ. A new methodology for analysis of creep and creep fracture data for 9–12% chromium steels. Inter Mater Ver. 2008. 53: 91-104.

- 4 Harrison W, Whittaker M, Williams S. Recent Advances in Creep Modelling of the Nickel Base Superalloy – Alloy 720Li. *Materials*. 2013. 6: 1118-1137.
- 5 Viswanathan R. *Damage Mechanisms and Life Assessment of High-Temperature Components*, ASM International, Palo Alto, CA, USA, 1993.
- 6 Penny RK, Mariott DL. *Design for Creep*. Chapman and Hall, 2nd Edition, Padstow-UK, 1995.
- 7 Dieter GE, Bacon D – *Mechanical Metallurgy*. McGraw-Hill Book Company, 1988.
- 8 Furtado HC, Almeida LH, LeMay I. Damage and remaining life estimation in high temperature plant with variable operating condition. *Ohmni*. 2008. 5: 1-1. Issue 1-May 2008-www.ohmni.co.uk.
- 9 NIMS-National Institute for Materials Science, Japan. NIMS Creep Data Sheet No.1B Data sheets on the elevated temperature properties of 1Cr0.5Mo steel tubes for boilers and heat exchangers. 1996.
- 10 Wilshire B, Scharring PJ. Extrapolation of creep life data for 1Cr– 0.5Mo steel. *International Journal of Pressure Vessels and Piping*. 2008. 85: 739– 743.